J. Membrane Biol. 170, 51–66 (1999)

The Journal of
Membrane
Biology

Rescue of Dysfunctional ΔF508-CFTR Chloride Channel Activity by IBMX

B.D. Schultz[1], **R.A. Frizzell**[2], **R.J. Bridges**[2]

[1]Department of Anatomy and Physiology, Kansas State University, Manhattan, KS 66506, USA

[2]Cystic Fibrosis Research Center and Department of Cell Biology and Physiology, University of Pittsburgh, Pittsburgh, PA 15261, USA

Received: 5 February 1999/Revised: 25 March 1999

Abstract. Nucleotide-dependent gating of ΔF508-CFTR was evaluated in membrane patches excised from HEK 293 and mouse L-cells and compared to observations on *wt*-CFTR channels recorded in the same expression systems. ΔF508-CFTR exhibited PKA activated, ATP-dependent channel gating. When compared to *wt*-CFTR, the K_m for ATP was increased by ninefold (260 μM *vs.* 28 μM) and maximal open probability (P_o) was reduced by 49% (0.21 ± 0.06 *vs.* 0.41 ± 0.02). Additionally, in the absence of PKA, ΔF508-CFTR inactivated over a 1 to 5 min period whereas *wt*-CFTR remained active. Time-dependent inactivation could be mimicked in *wt*-CFTR by the intermittent absence of ATP in the cytosolic solution. The effects of 3-isobutyl-1-methyl xanthine (IBMX), a compound reported to stimulate ΔF508-CFTR, were evaluated on *wt*- and ΔF508-CFTR channels. At concentrations up to 5 mM, IBMX caused a concentration dependent reduction in the observed single channel amplitude (*i*) of *wt*-CFTR (maximal observed reduction 35 ± 3%). However, IBMX failed to significantly alter total patch current because of a concomitant 30% increase in P_o. The effects of IBMX on ΔF508-CFTR were similar to effects on *wt*-CFTR in that *i* was reduced and P_o was increased by similar magnitudes. Additionally, ΔF508-CFTR channel inactivation was dramatically slowed by IBMX. These results suggest that IBMX interacts with the ATP-bound open state of CFTR to introduce a short-lived nonconducting state which prolongs burst duration and reduces apparent single channel amplitude. A secondary effect observed in ΔF508-CFTR, which may result from this interaction, is a prolongation of the activated state. In light of previously proposed linear kinetic models of CFTR gating, these results suggest that IBMX traps CFTR in an ATP-bound state which may preclude inactivation of ΔF508-CFTR.

Key words: Cystic fibrosis — Chloride channel — Kinetics — ΔF508-CFTR — Nucleotide

Introduction

The product of the gene which, when mutated, causes cystic fibrosis codes for an integral membrane protein (the cystic fibrosis transmembrane conductance regulator; CFTR[1]) which is a small (6–11 pS), ohmic, chloride-conducting channel (Berger et al., 1991). Functional integrity of this channel is required for the transport of chloride across epithelial barriers resulting in salt and fluid secretion or absorption (Welsh & Smith, 1993). The most common mutation in CFTR, ΔF508, is associated with at least two defects. The first is that the ΔF508-CFTR protein is not trafficked correctly to the cell membrane (Cheng et al., 1990), a defect which has been overcome in some in vitro systems (Denning et al., 1992; Brown et al., 1996; Sato et al., 1996). Once the ΔF508-CFTR protein arrives at the cell membrane, most reports indicate that channel activity differs from that of *wt*-CFTR. Whole-cell and single channel kinetics are reported to be affected, but questions remain regarding which parameter or biophysical state is most changed (Dalemans et al., 1991; Drumm et al., 1991; Sherry, Cup-

Correspondence to: B.D. Schultz

[1] Nonstandard Abbreviations: CF, cystic fibrosis; CFTR, cystic fibrosis transmembrane conductance regulator; PDE, phosphodiesterase; f_c, corner frequency; *i*, single channel current; *I*, mean patch current; IBMX, 3-isobutyl-1-methyl xanthine; *N*, number of channels present in a membrane patch; NBD, nucleotide binding domain; P_o, open probability; R-domain, regulatory domain; S_o, low frequency power of Lorentzian function; *wt*, wild type

poletti & Malinowska, 1994; Haws et al., 1996; Becq et al., 1996; Sato et al., 1996; Hwang et al., 1997). These observations could reflect changes in phosphorylation-dependent activation/inactivation and/or changes in nucleotide-dependent gating kinetics. Alternatively, two reports have concluded that gating kinetics are not greatly affected by the ΔF508 mutation (Li et al., 1993; Pasyk & Foskett, 1995).

3-Isobutyl-1-methyl xanthine (IBMX) is one of many compounds that have now been reported to stimulate ΔF508-CFTR-mediated chloride conductance (Drumm et al., 1991; Becq et al., 1993; Yang et al., 1993; Haws et al., 1996). Well documented effects of IBMX on the activity of intracellular enzymes including alkaline phosphatase (Croce, Kramer & Garbers, 1979; Farley, Ivey & Baylink, 1980) and phosphodiesterase (Beavo et al., 1970) are thought to account for these effects on *wt*-CFTR-mediated ion transport. However, significant stimulation of ΔF508-CFTR chloride conductance is seen only at concentrations far in excess of concentrations expected to affect these intracellular enzymes and in excess of those which fully stimulate *wt*-CFTR in the same expression systems. At the higher concentrations, the mechanism of stimulation remains unresolved. Effects of IBMX on CFTR, independent of alterations in cAMP concentrations, have been reported (Cohen et al., 1997; He et al., 1998). Information regarding the mechanism of action of IBMX might provide insights into the underlying differences in the gating of *wt*- and ΔF508-CFTR.

Therefore, experiments were conducted to determine which kinetic parameters of CFTR were most affected by the ΔF508 mutation in cell-free membrane patches and to determine if IBMX caused a direct effect on ΔF508-CFTR channel activity that could account for the favorable changes in macroscopic current levels that have been reported. Results suggest that IBMX directly interacts with CFTR to introduce a novel kinetic state and thus, favorably alters the state distribution of ΔF508-CFTR to provide for prolonged channel activity. Some of these data have previously been presented in abstract form (Schultz, Bridges & Frizzell, 1994; Schultz, Frizzell & Bridges, 1994).

Materials and Methods

Patch-clamp experiments were performed using excised inside-out membrane patches from HEK 293 and L-cells expressing either *wt*- or ΔF508-CFTR. Channel activity in the two expression systems was indistinguishable. The data were acquired and analyzed as described previously (Venglarik et al., 1994) with minor modifications. All experiments were performed at 34 to 37°C unless otherwise stated with membrane potential held at −60 or −80 mV (bath *vs.* pipette) so that negative currents (represented as downward deflections) represent chloride channel openings. Cells were exposed to forskolin (2–5 μM) to endogenously phosphorylate CFTR prior to patch excision into a bath which contained ATP. In most patches, the catalytic subunit of cyclic AMP dependent protein kinase (PKA; Promega, Madison, WI) was added to the bath following patch excision to insure and/or maintain maximal CFTR channel activation. Unless otherwise noted, the 0.75 ml bath was refreshed at a rate of 4 bath volumes per min during the control and treatment periods. Recordings of up to 25 min in length were analyzed for each membrane patch. Single channel current (*i*) was determined based on fits of multi-Gaussian functions to amplitude histograms of the current records without constraining the peak amplitudes to be equally spaced and thus further document that a homogenous population of channels was being evaluated. Mean channel amplitude during each treatment period (e.g., duration of exposure to a unique combination of stimulants or at a given holding potential) was calculated as the average distance between peaks. Mean current (*I*) was determined by averaging all data points in the current record during the treatment period. Current records were visually examined for the duration of patch viability to determine the number of actively gating channels (*N*) present in the patch (i.e., the maximum number of channels simultaneously open in conditions that maximize channel activity; e.g., ≥1 mM ATP with PKA; (Horn, 1991; Venglarik et al., 1994). Values of *i*, *I*, and *N* were used to calculate the channel P_o from the equation $P_o = I\,(Ni)^{-1}$. Only patches containing less than eight channels were evaluated for statistical analysis of P_o (Venglarik et al., 1994). Fluctuation analysis and estimation of the corner frequency (f_c), were performed using Bio-Patch software (version 3.30; Molecular Kinetics, Pullman, WA) as previously described (Venglarik et al., 1994). Nonlinear fits to the data for concentration-response relationships were completed using SigmaPlot (for Windows, version 4.0; Jandel Scientific, San Rafael, CA). Values are presented as the mean and SEM. Paired *t*-tests were performed using SigmaPlot to determine significance of treatment effects. Effects are considered significant if $P < 0.05$ for type I errors.

Cell Culture

L-cells, a murine fibroblast cell line, stably expressing either *wt*- or ΔF508-CFTR were maintained as previously described (Yang et al., 1993). Briefly, cells were grown in Dulbecco's modified Eagle's medium (GIBCO BRL, Gaithersburg, MD) supplemented with 10% fetal bovine serum, 100 u ml^{-1} penicillin and 100 μg ml^{-1} streptomycin. Cells were passaged twice weekly. For patch-clamp studies, cells were plated onto plastic coverslips coated with human placental collagen (collagen type VI; Sigma, St. Louis, MO) and channel activity was evaluated 2 to 4 days after plating.

HEK 293 Cells. *wt*- or ΔF508-CFTR cDNA was cloned into pCMVβ (Clontech, Palo Alto, CA) in place of the β-galactosidase gene and thus obtain the pCMV/wt/CFTR or pCMV/ΔF508/CFTR constructs. HEK 293 cells were seeded on plastic coverslips coated with human placental collagen in 35 mm dishes at density of 40–50%. On the following day, cells were transfected with 5 μg/dish plasmid DNA by calcium phosphate coprecipitation method as previously described (Graham & van Der Eb, 1973). Cells were maintained in standard incubation conditions and channel activity was evaluated 2 days later.

Single Channel Recording and Analysis

The analogue recording and digital acquisition apparatus were as previously described (Schultz et al., 1995; Venglarik et al., 1994). In general, digitized files were acquired at a sampling rate of 400 Hz (low-pass 8 pole Bessel filter at 200 Hz; 902LPF, Frequency Devices, Haverhill, MA) and analyzed using Bio-Patch software as previously described with the exception that the power density spectra (PDS) were examined to an upper frequency of 140 Hz. For clarity of presentation, most data are plotted at a frequency of 200 Hz. Some records (e.g., Fig.

5*B*) were acquired at sampling frequencies of up to 2 kHz (low-pass filtered at 800 Hz) for presentation and to determine if additional Lorentzian components could be identified in this portion of the spectra. For analysis, all data points form a treatment period were included in the construction of amplitude histograms. However, for presentation, data sets were restricted to 60 or 120 seconds duration so that the area under the fitted curves could be directly compared.

For experiments to determine the longevity of channel activity and stability of P_o, L-cells expressing *wt*- or ΔF508-CFTR were exposed to 5 μM forskolin and patches were excised into a bath containing various concentrations of ATP, PKA, and IBMX. Channel activity was recorded until patch membranes broke; for these data sets, most patches were maintained for at least 7 min. To ascertain if the loss of observed channel activity was due to incremental diminution in P_o or to channel inactivation, P_o of channels was determined for each patch over 30-sec periods. For these studies, channel activity was analyzed using the following criteria. When actively gating channels were no longer observed in a patch, the patch was designated as 'nonviable' and records subsequent to the last observed event were excluded from analysis. This method is conservative in that it will designate [viable] patches with inactive channels as being nonviable (i.e., P_o is undetermined rather than zero). The maximum number of channels observed during the entire recording, along with single channel amplitude and mean current were used to determine P_o during each successive 30-sec interval during which channels remained active.

Solutions

The pipette solution contained (in mM): 140 N-methyl-D-glucamine-HCl (NMDG-Cl), 1 $CaCl_2$, 2 $MgCl_2$, 10 1,3-bis[tris(hydroxymethyl)-methylamino]propane-HCl (BTP). The bathing solution contained (in mM): 150 NaCl, 2 $MgCl_2$, 10 NaF, 0.5 ethylene glycol-bis(β-aminoethyl ether) N,N,N′,N′-tetraacetic acid (EGTA), 0.26 $CaCl_2$, and 10 BTP. The pH of both the bath and pipette solutions was maintained between 7.33 and 7.37 in all experiments. Free Ca^{2+} concentration in the bath was calculated to be 100 nM (Brooks & Storey, 1992). Fluoride was included as a nonspecific inhibitor of any phosphatases that might be present at excision and can lead to channel inactivation (Tabcharani et al., 1991). We have previously evaluated *wt*-CFTR channel activity in the presence and absence of F^- and could identify no difference in kinetic behavior (Schultz et al., 1995; Schultz, Bridges & Frizzell, 1996). The disparity in this regard with the report by Berger, Travis and Welsh (1998) is at this time unexplained.

ATP was made as a stock solution (200 mM) in 200 mM BTP and the pH adjusted to 7.2. Aliquots were frozen at −20°C until use.

Chemical Sources

Na_2ATP was obtained from Boehringer Mannheim (Indianapolis, IN). Forskolin (*Coleus forskohlii*) was purchased from Calbiochem (La Jolla, CA). The catalytic subunit of cyclic-AMP-dependent protein kinase (PKA) was obtained from Promega (Madison, WI). IBMX was purchased from Sigma. All other chemicals used were reagent grade.

Results

ΔF508-CFTR Channel Activity is Regulated by Phosphorylation and Nucleotides

A continuous recording of a membrane patch excised from an HEK 293 cell containing at least 15 ΔF508-CFTR Cl^- channels is presented in Fig. 1. Prior to patch excision, the cell was exposed to forskolin to stimulate PKA activity and F^- was present as a nonspecific phosphatase inhibitor throughout the entire experiment. Upon excision into a static bath containing 300 μM ATP, a maximum of 2 simultaneously open channels was observed. PKA catalytic subunit (200 u ml^{-1}) was then added to the solution bathing the cytosolic face of the membrane to activate (phosphorylate) the ΔF508-CFTR channels. Up to 9 simultaneously open channels were then observed. An increase in ATP concentration to 3 mM caused a further increase in the number of simultaneously open ΔF508-CFTR channels to 15. The solution bathing the intracellular face of the membrane was then replaced by continuous perfusion with a bath containing no PKA and 300 μM ATP. Washout of PKA and reduction of ATP concentration was accompanied by an immediate reduction in current and a loss of channel activity. The results presented in Fig. 1 demonstrate that the ΔF508-CFTR regulation is qualitatively similar to observations regarding kinase- and nucleotide-dependent regulation of *wt*-CFTR activity.

Dependence of ΔF508-CFTR P_o on ATP Concentration

Shown in Fig. 2*a* are excerpts of representative current records of membrane patches excised from L-cells containing 3 ΔF508-CFTR Cl^- channels. PKA (200 u ml^{-1}) was present in a static bath solution during these recordings. For the three records shown, ΔF508-CFTR channel P_o ranged from 0.09 in the presence of 300 μM ATP to 0.20 in the presence of 3 mM ATP. Amplitude histograms show that *i* was not affected by differences in ATP concentration. The data from these and additional experiments demonstrate that, in the presence of PKA, the P_o of ΔF508-CFTR channels depends on the concentration of ATP present at the cytosolic face of the membrane. These and similar results from a total of 52 excised membrane patches are summarized in Fig. 2*B*. Results from parallel experiments employing L-cells expressing *wt*-CFTR are included for comparison. A Michaelis-Menten type saturation function for a simple bimolecular reaction was fitted to each set of observations to quantitate differences in nucleotide dependencies. The $P_{o\,max}$ derived for ΔF508-CFTR was half that of *wt*-CFTR (0.21 ± 0.06 *vs.* 0.41 ± 0.02) and K_m was right-shifted by 9-fold (260 ± 190 μM *vs.* 28 ± 8 μM).

ΔF508-CFTR Loses Activity Over Time

Previously we reported that *wt*-CFTR routinely remains active in excised membrane patches in the absence of PKA (Venglarik et al., 1994; Schultz et al., 1995). However, in acquiring and compiling the data presented in

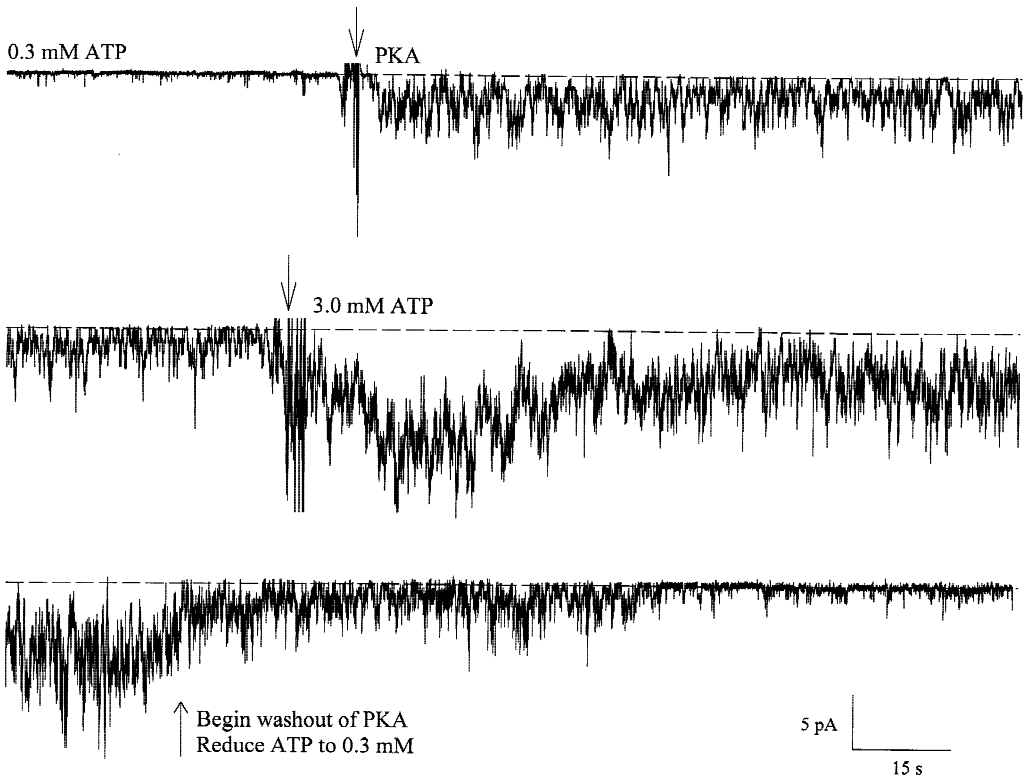

Fig. 1. ΔF508-CFTR channel activity requires phosphorylation by PKA and the ongoing presence of ATP. Shown is a continuous recording of a membrane patch excised from an HEK 293 cell containing at least 15 ΔF508-CFTR Cl^- channels. The patch was excised into a static bath containing 300 μM ATP. PKA catalytic subunit (200 u ml^{-1}) and ATP (to 3 mM) were added to the solution bathing the cytosolic face of the membrane, as indicated. The solution bathing the intracellular face of the membrane was then replaced by continuous perfusion with a bath containing no PKA and 300 μM ATP. The dashed lines indicate the current level when all channels were closed.

Fig. 2, it became obvious that ΔF508-CFTR channels did not share this attribute; channel activity decreased over the time of recording. An example of this 'run down' is presented in Fig. 1 and evidence documenting the 'run down' is presented in Fig. 3. As shown in Fig. 3*A*, ΔF508-CFTR channel activity ended in many patches during the recording period. Within two minutes after excision of patches containing actively gating ΔF508-CFTR into a bath containing 1 mM ATP, channel activity was no longer observed in more than 50% of patches (6 of 10); activity was not observed in any patch more than five minutes following excision. Alternatively, excision into a bath containing 200 u ml^{-1} PKA increased the likelihood that ΔF508-CFTR channels would continue to actively gate for five minutes or more; channel activity was observed in more than half the patches (7 of 12) six minutes after excision. For comparison, *wt*-CFTR channels remained active throughout the recording period in all patches observed (11 of 11), in the absence of PKA. As shown in Fig. 3*B*, the P_o of ΔF508-CFTR never reached the same level as *wt*-CFTR recorded in the same conditions, although the P_o of channels in active patches remained relatively stable for both constructs. Since, after the 5 min time point, ΔF508-CFTR channel activity was not observed in the absence of PKA, one cannot be assured that channels were present, but with a P_o of zero as opposed to recording failures due to other limitations i.e., nonviable patches. That P_o did not substantially decline in patches with actively gating channels, but that the number of patches with active channels was reduced over the duration of the recordings (Fig. 3*A*) suggests that ΔF508-CFTR channels were inactivating rather than exhibiting incremental reductions in P_o. Excision of patches containing ΔF508-CFTR into a bath containing PKA (200 u ml^{-1}), was associated with an extended duration of channel activity and P_o was relatively stable throughout the recording period (the modest downward trend in P_o could result from the inactivation of individual channels in multichannel patches that would have led to an apparent reduction in P_o for the remaining active channels in that patch). P_o of *wt*-CFTR was greater than that of ΔF508-CFTR at all time points and remained relatively stable throughout the recordings. These results demonstrate that, even in the most favorable conditions tested (1 mM ATP and PKA), ΔF508-CFTR has a lower P_o than *wt*-CFTR and channel activity is not as stable in the absence of kinase activity. Because truly stationary kinetics were not routinely observed, es-

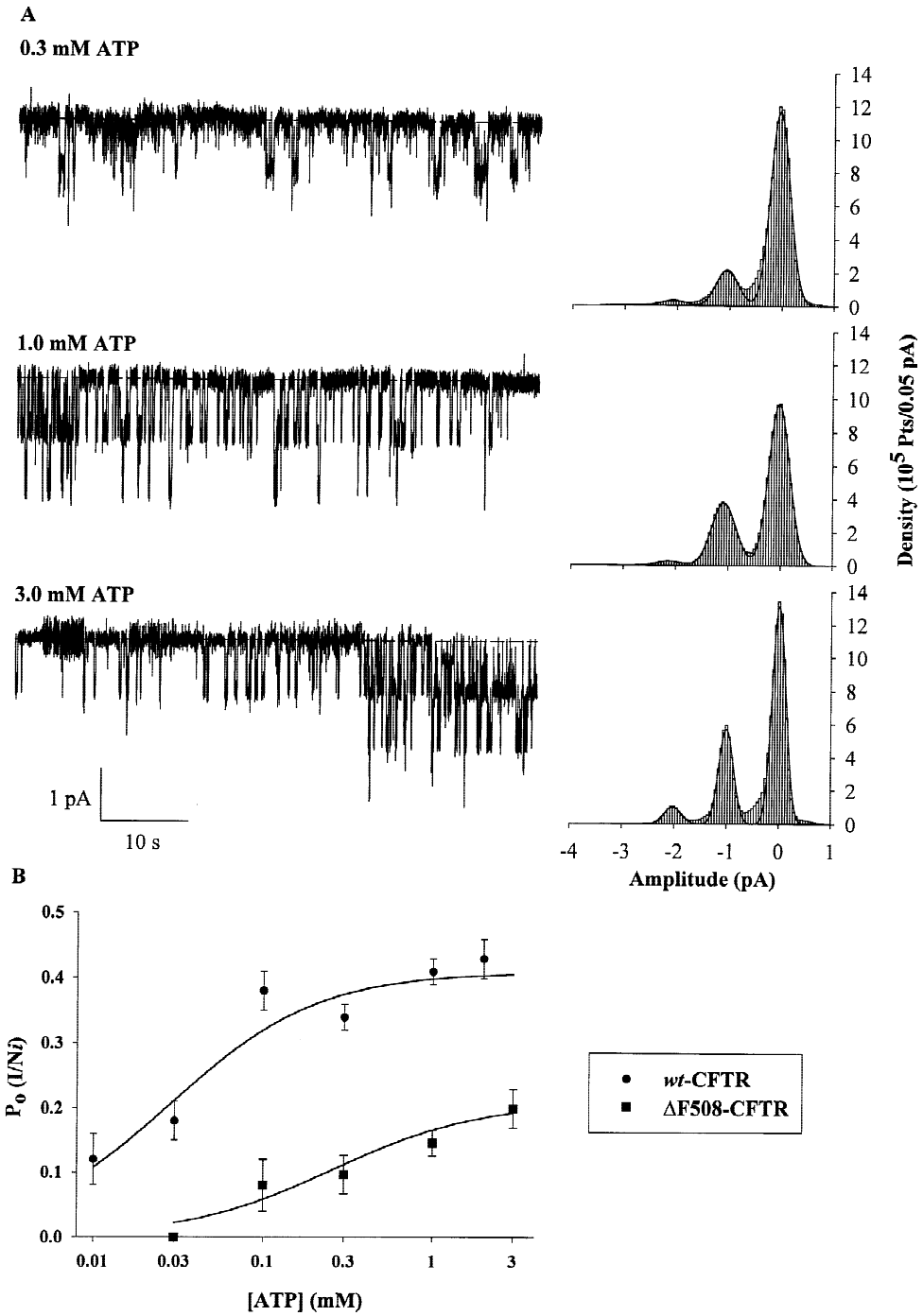

Fig. 2. ΔF508-CFTR channel P_o depends on ATP in a concentration dependent manner. (*A*) Membrane patches containing a maximum of three simultaneously open channels were excised from L-cells into baths containing PKA (200 u ml^{-1}) and various concentrations of ATP as indicated. The dashed lines indicate the current level when all channels were closed. (*B*) ATP concentration dependence of *wt*- and ΔF508-CFTR Cl^- channel P_o. P_o was calculated using the equation as shown in the axis title where *I* was the mean current during the duration of the observation, *N* was the maximum number of simultaneously open channels observed in the patch, and *i* was the single channel amplitude. Conditions were as described in Panel *A* except that observations on *wt*-CFTR were made in the absence of PKA. Means ± SEM are shown for 12 to 44 observations at each concentration with the exception of 0.03 and 0.1 mM with the ΔF508-CFTR where 1 and 3 observations were made, respectively. Solid lines indicate the best fit of a Michaelis-Menten type saturation function for a simple bimolecular reaction to the observations. The data sets include 147 and 66 observations for *wt*- and ΔF508-CFTR, respectively.

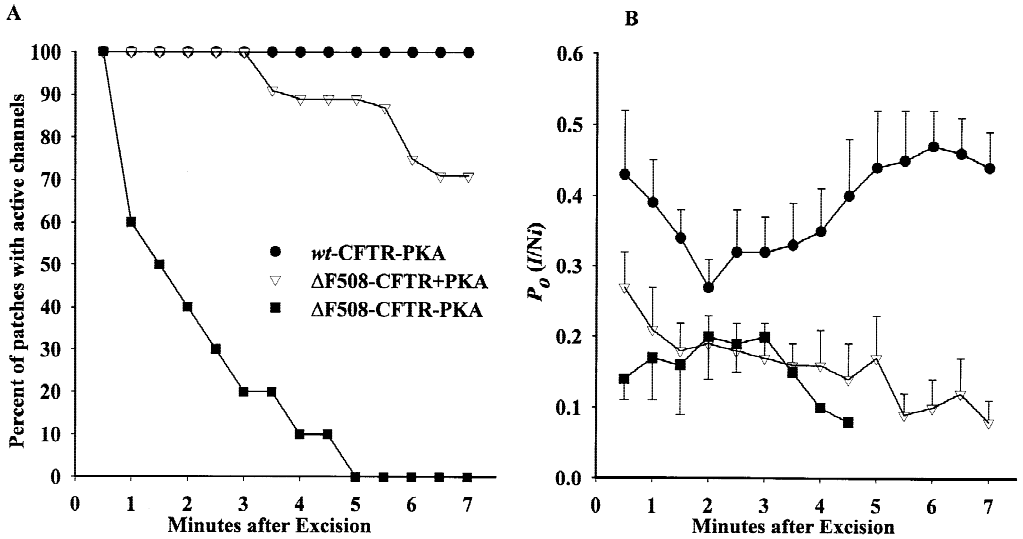

Fig. 3. Time dependence of *wt*- and ΔF508-CFTR channel activity. (*A*) Percentage of patches with channels remaining active over time. (*B*) Comparison of channel P_o in the presence of 1 mM ATP and the presence or absence of PKA (200 u ml^{-1}). P_o was calculated as described in Fig. 2. P_o for channels within each patch were calculated over 30-sec intervals and averaged over all patches. Ten to twelve patches were evaluated for each data set. Means ± SEM are displayed for each data point. SEM could not be determined when the number of patches with actively gating channels fell below three.

timates of the nucleotide-dependent opening rate and the closing rate could not be made with a high degree of confidence and estimates of kinetic parameters must be viewed as 'first approximations.' Specifically, the K_m for nucleotide dependence of ΔF508-CFTR channel P_o presented in Fig. 2*B*, must be viewed as a 'best estimate' within these limitations.

wt-CFTR Channels Inactivate When Deprived of ATP

Results presented in Fig. 4 are from experiments designed to determine if there might be a causal relationship between occupancy of ATP binding domain(s) and the stability of actively gating channels. In panel *A* are shown excerpts from a continuous record of an excised membrane patch containing at least 7 *wt*-CFTR channels. Initially upon excision, the bath solution contained 300 μM ATP. The inflowing solution was changed to one which contained no ATP for one minute. During this time, P_o declined to zero as shown. ATP was then reintroduced into the bath (for a total of 120 seconds) and channels again began to actively gate. However, the average current and the maximal number of open channels was reduced when compared to the previous period during which ATP was present. ATP was again omitted from the inflowing solution, but for a three-minute period followed by reintroduction. During the final exposure to ATP, the maximal number of simultaneously observed channels was reduced to three and *I* was 0.8 pA. These results and those of eight similar experiments are summarized in Fig. 4*B*. Results indicate that, when compared to the previous period during which ATP was present, *I* and N_{obs} were inversely proportional to the duration during which ATP was absent from the bath solution. In five of the nine patches employed for this set of experiments, PKA was added (in the presence of ATP) after channels had inactivated. This treatment resulted in an increase in the number of active channels compared to the previous recording period which further suggests that channels had, in fact, dephosphorylated (inactivated) during the course of the recording in which ATP was only intermittently present (*data not shown*).

IBMX Causes a Fast Block of *wt*-CFTR

We first determined if IBMX affected the gating kinetics of *wt*-CFTR in excised membrane patches. As shown in Fig. 5, IBMX, at the concentrations reported to increase mutant CFTR Cl^- conductance in *Xenopus* oocytes (Wilkinson et al., 1996), alters the gating behavior of *wt*-CFTR. In this example, an excised membrane patch which contained three actively gating CFTR Cl^- channels was observed in control conditions and in the presence of IBMX (1 and 5 mM). In control conditions, a multi-Gaussian function fitted to the amplitude histogram revealed that $i = 1.07$ pA. Channels exhibited gating kinetics that are similar to those which we previously reported (Fig. 5*A* and *B;* (Venglarik et al., 1994; Schultz et al., 1995). Fluctuation analysis (Fig. 5*D*), likewise, supported previous observations demonstrating a Lorentzian component associated with nucleotide-

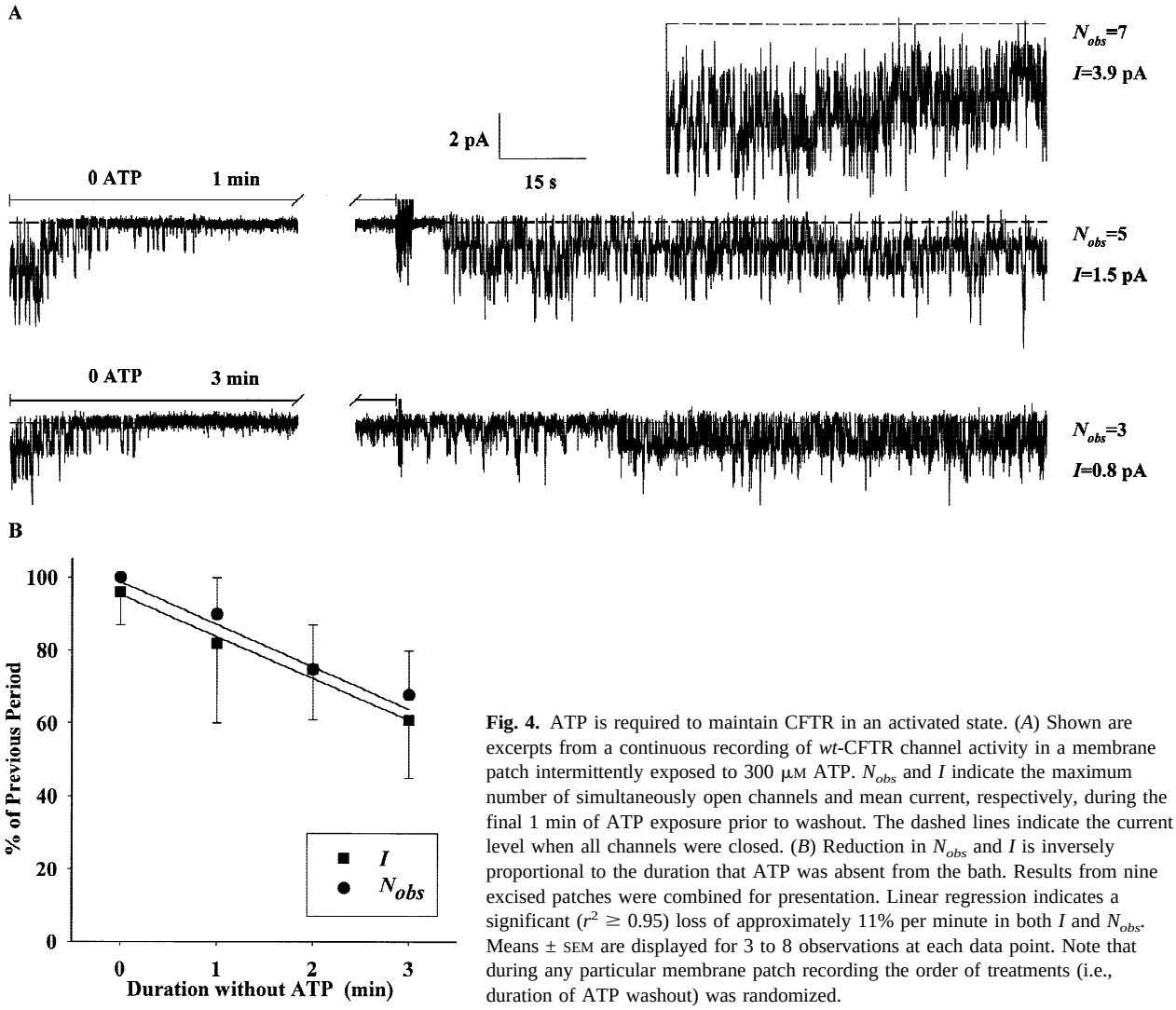

Fig. 4. ATP is required to maintain CFTR in an activated state. (*A*) Shown are excerpts from a continuous recording of *wt*-CFTR channel activity in a membrane patch intermittently exposed to 300 μM ATP. N_{obs} and *I* indicate the maximum number of simultaneously open channels and mean current, respectively, during the final 1 min of ATP exposure prior to washout. The dashed lines indicate the current level when all channels were closed. (*B*) Reduction in N_{obs} and *I* is inversely proportional to the duration that ATP was absent from the bath. Results from nine excised patches were combined for presentation. Linear regression indicates a significant ($r^2 \geq 0.95$) loss of approximately 11% per minute in both *I* and N_{obs}. Means ± SEM are displayed for 3 to 8 observations at each data point. Note that during any particular membrane patch recording the order of treatments (i.e., duration of ATP washout) was randomized.

dependent bursts (f_c = 1.63 Hz; S_o = 0.20 pA^2 sec^{-1}) and a second Lorentzian component associated with short-lived closures within a burst (f_c = 64 Hz; S_o = $1.7 \cdot 10^{-4}$ pA^2 sec^{-1}). Addition of 1 mM IBMX to the solution bathing the intracellular face of the membrane caused a modest change in gating kinetics (Fig. 5A and B). In the presence of IBMX, the open channel noise is increased and additional short-lived, poorly resolved transitions to a nonconducting state are observed. In this figure, the gating change is more obvious at the single open level in the higher resolution trace (Panel *B*) where numerous short-lived transitions to the closed state are seen. Noise observed while all channels were closed was not affected by IBMX addition. The effect of 1 mM IBMX on CFTR is perhaps most apparent on inspection of the amplitude histogram (Fig. 5*C*). The width of the distribution about the closed level is not changed (Standard deviation control 0.11 pA; 1 mM IBMX, 0.10 pA). However, peaks associated with open channel levels are broadened (e.g., standard deviation of the distribution for the first open level increased from 0.13 pA to 0.28 pA) and *i* was reduced to 0.93 pA. *I* was little changed by 1 mM IBMX (0.62 pA). Fluctuation analysis revealed that 1 mM IBMX caused a reduction in the power associated with nucleotide-dependent gating from 0.21 to 0.14 pA^2 sec^{-1} with a concomitant increase in f_c to 1.68 Hz (*data not shown*). A further increase in IBMX concentration to 5 mM heightened the observed effects. Inspection of current record at higher resolution (Fig. 5*B*) reveals greater noise associated with the open state and greater difficulty in resolving openings to the second or third level. A multi-Gaussian function fitted to the amplitude histogram indicated a further diminution in *i* to 0.67 pA (Fig. 5*C*). Again, note that the distribution about the closed state is not changed (standard deviation 0.10 pA), but that the distribution about the open state is sufficiently broadened to obscure a clear peak for the levels associated with the second and third open channels. *I* was only

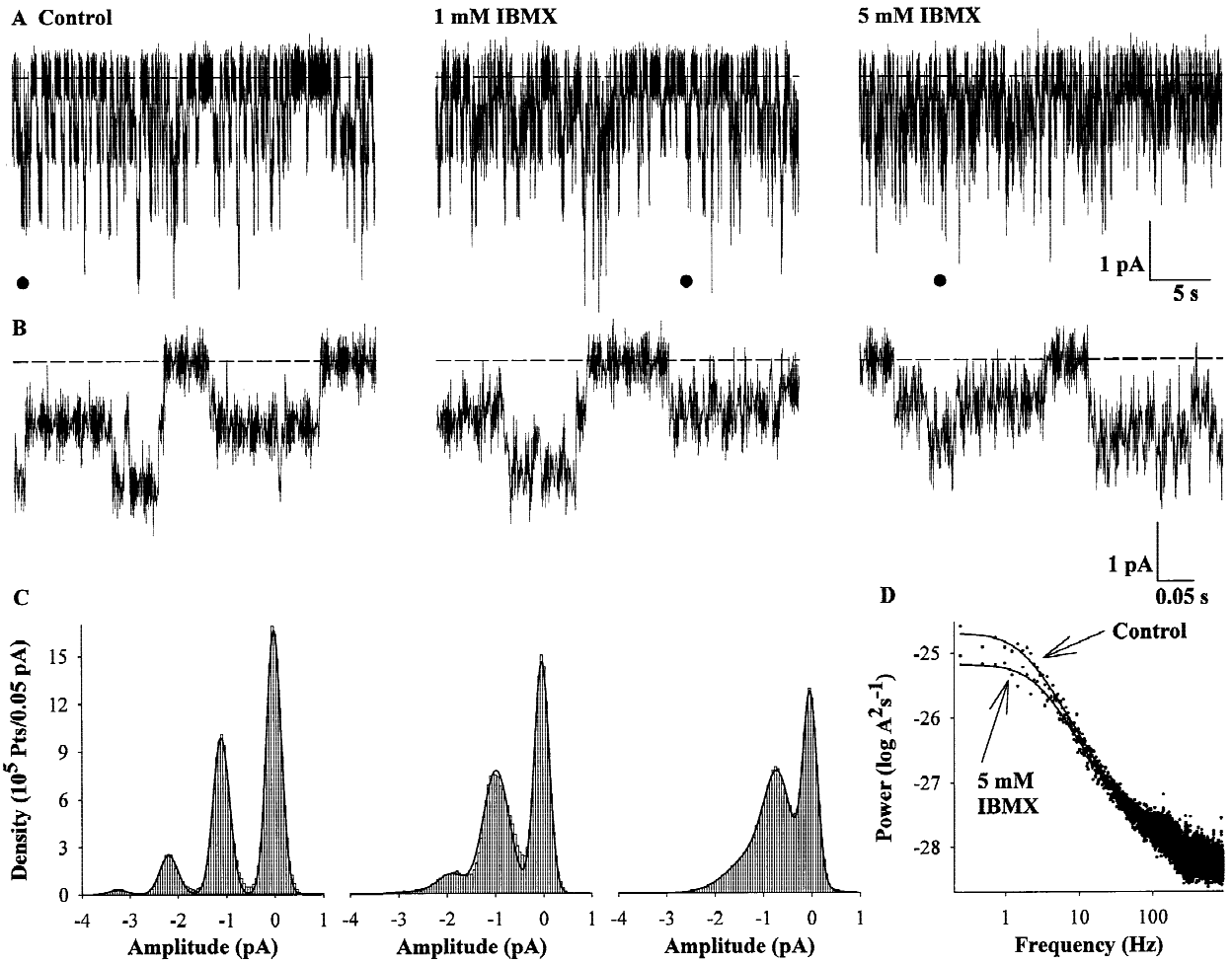

Fig. 5. IBMX-induced changes in *wt*-CFTR Cl^- channel activity. (*A*) Low resolution (sampling rate = 200 Hz) and (*B*) high resolution (sampling rate 2000 Hz) panels are excerpts from a continuous current record of a membrane patch excised from a CFTR transfected L-cell. The concentration of IBMX present at the intracellular face of the membrane was as indicated. Filled circles indicate that portion of the recording in panel *A* which is expanded for presentation in panel *B*. The dashed lines indicate the current level when all channels were closed. (*C*) Amplitude histograms constructed using 1 min of continuous current record in each of the three conditions, respectively. (*D*) Power density spectra constructed from 29 and 20 nonoverlapping data segments digitized at 2000 Hz after passing through a low-pass 8-pole Bessel filter (cutoff frequency 800 Hz). A multi-Lorentzian function was fitted to each data set. Parameters of each fitted line are presented in the text.

slightly reduced by 5 mM IBMX (0.59 pA). Fluctuation analysis (Fig. 5*D*) indicated that 5 mM IBMX caused a further reduction in the power of the nucleotide-dependent Lorentzian component to 0.067 pA^2 sec^{-1} with a further increase in f_c to 2.54 Hz. Although obscured by the number of data points, a second effect of IBMX was to increase the f_c of the high-frequency Lorentzian component. In this example, f_c was 64, 97, and 180 Hz for control, 1 and 5 mM IBMX, respectively, although the power associated with this Lorentzian component did not change ($1.7 \cdot 10^{-4}$ pA^2 sec^{-1}) with increases in IBMX concentration. This change in the PDS is consistent with an IBMX-induced increase in the number of short-lived closures within a burst. These data along with data gathered in similar experiments are summarized in the Table. These data show that IBMX significantly reduces *i*, but increases P_o such that *I* is unchanged. These results are consistent with the effect of IBMX being to prolong the open state by punctuating it with many short-lived, unresolved closures.

Although not separated for individual presentation, experiments designed to evaluate the effects of IBMX on CFTR were completed in various concentrations of ATP (0.1, 0.3, 0.6, 1.0, 3.0, 10.0 mM) and at −60 and −80 mV. Changes in ATP concentration did not alter the concentration-dependent effects of IBMX on CFTR channel activity. In every case, IBMX caused a statistically significant reduction in *i*, an increase in open channel noise, no

Table. Effects of IBMX on *wt*-CFTR channel amplitude (*i*), patch current (*I*) and open probability (P_o)

[IBMX] (mM)	*i* (pA @ −80 mV)	Δ*I* (% change from control)	P_o
0.0 (Control)	1.08 ± 0.01 (18)[a]		0.29 ± 0.03 (26)
0.5	1.06 ± 0.02[b] (4)	18 ± 22 (4)	0.32 ± 0.03 (4)
1.0	0.93 ± 0.02[b] (7)	−12 ± 10 (13)	0.33 ± 0.05 (11)
5.0	0.67 ± 0.03[b] (7)	−3 ± 13 (11)	0.38 ± 0.06[b] (11)

[a] Mean ± SEM; Numbers in parentheses indicate the number of observations included in the reported mean. ATP (0.3 mM) was present during all recordings.
[b] Significantly different from paired control.

consistent effect on *I*, and an apparent increase in P_o that reached statistical significance only in 5 mM IBMX. Three additional experiments were conducted to further investigate the possibility that IBMX-induced effects were voltage dependent. As shown in Fig. 6, current-voltage relationships were constructed based upon current records from three excised membrane patches made in the absence and presence of 5 mM IBMX. Results show that single channel conductance is similarly affected at all potentials, which included observations at positive potentials and with outward currents. IBMX (5 mM) reduced the slope conductance from 11.8 pS to 7.7 pS.

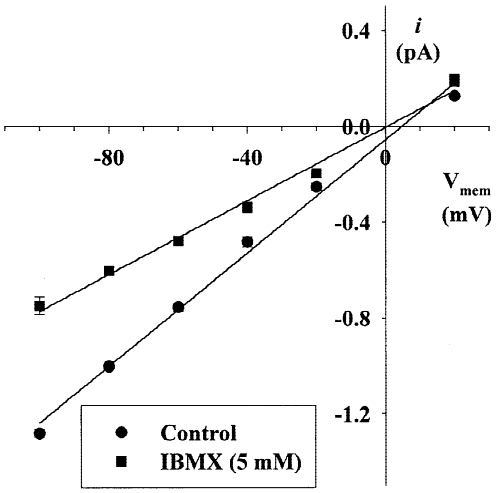

Fig. 6. Current-voltage relationship for *wt*-CFTR Cl^- channels in the absence and presence of 5 mM IBMX. Slope conductance and reversal potential were 11.8 pS and 4.7 mV in control conditions, and 7.7 pS and −0.27 mV in the presence of 5 mM IBMX.

IBMX Causes a Fast Block of ΔF508-CFTR

The effects of IBMX on ΔF508-CFTR were similar to the effects observed on *wt*-CFTR in that *i* was significantly reduced by the same magnitude and fluctuation analysis revealed similar IBMX-induced changes in gating frequency (data not shown). Shown in Fig. 7 are excerpts from a continuous recording of ΔF508-CFTR channel activity in the excised patch configuration. The patch was excised into a static bath which contained ATP (1 mM), IBMX (1 mM), and forskolin (2 μM). During the first ten minutes following excision, a maximum of one open level was observed and openings were infrequent ($P_o \ll 0.05$; Panel *A*). [It is important to note, however, ΔF508-CFTR remained active, albeit at low P_o; a stark contrast to previous recordings made in the absence of IBMX (e.g., *see* Figs. 1 and 2)]. PKA was then added to the static bath which caused channel activation and a maximum of 4 simultaneously open channels was observed ($N = 4$). Stable channel activity was observed in these conditions for over three minutes (Panel *B*) before the bath solution was changed by continuous perfusion to one which contained IBMX and ATP (1 mM, each), but did not include PKA.[2] During the following four minutes, channels continued to actively gate, although *I* decreased and the fourth open level was not seen during the final two minutes of this recording period (i.e., it appears that one of the channels inactivated/dephosphorylated; Panel *C*). The bath was then changed to include no IBMX, but still with 1 mM ATP. As expected, *i* immediately increased from 0.70 pA to 0.80 pA and open channel noise was reduced (Panel *D*). During this recording period (4 minutes) the third open level was observed only infrequently although it was observed throughout the entire period. Subsequently, the concentration of ATP was reduced to 300 μM with further reduction in *I*. Although the patch remained viable for only an additional two minutes, *I* and *N* continued to decline such that during the final thirty seconds of recording, *I* was ~0.15 pA and the third open level was not observed.

IBMX Contributes to the Maintenance of ΔF508-CFTR Channel Activity in Excised Patches

ΔF508-CFTR channel activity can be maintained for an extended period in the presence of IBMX. As shown in Fig. 7 channels remained active for more than ten min-

[2] The reduction in *i* that accompanied washout of PKA is likely accounted for by the perfusion solution being slightly cooler than the static bath solution. (Records of bath temperature were not kept for this experiment, however, we have previously reported the temperature-dependence of CFTR channel amplitude (Schultz et al., 1995)).

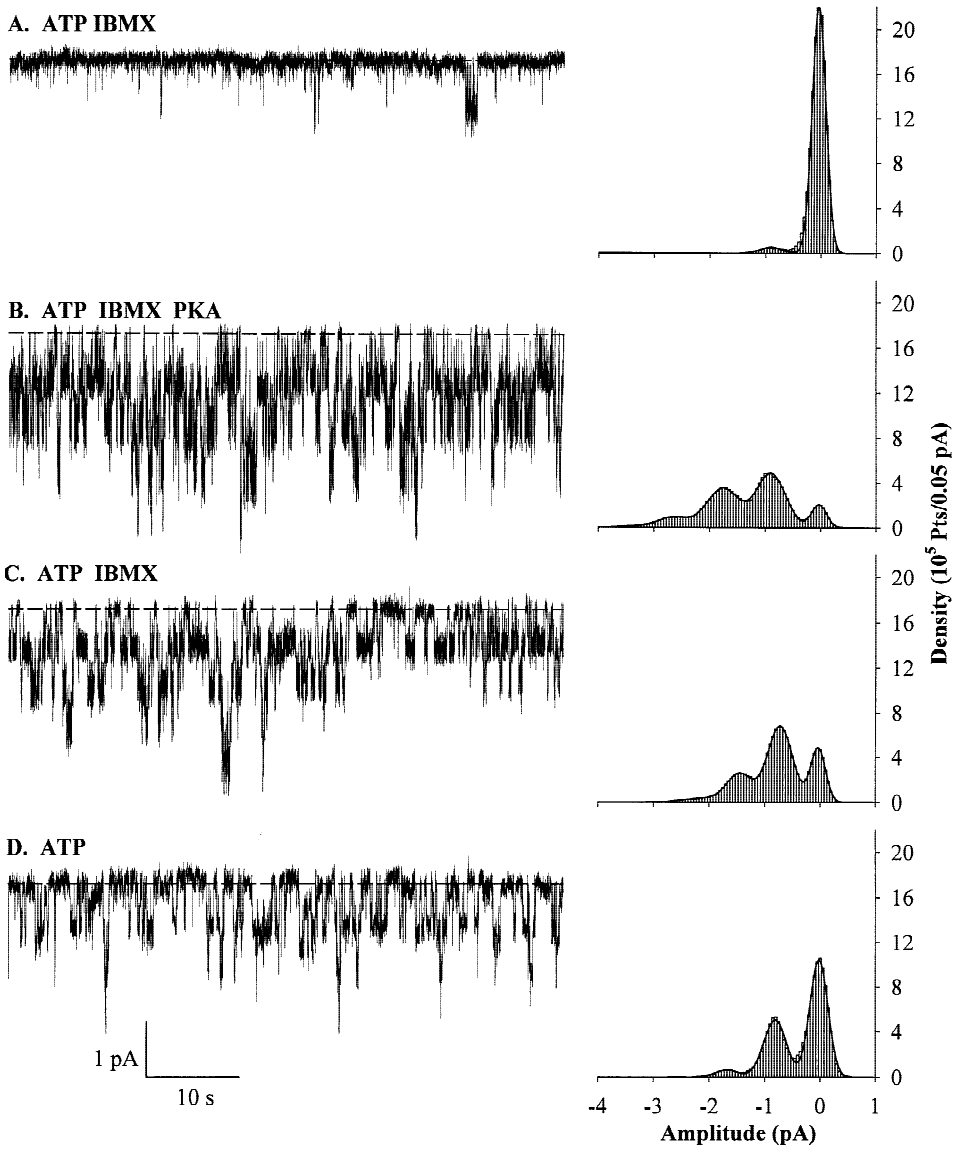

Fig. 7. IBMX prolongs activity and reduces amplitude of ΔF508-CFTR Cl^- channels. Shown are excerpts of a continuous record of ΔF508-CFTR Cl^- channel activity in an excised membrane patch and associated amplitude histograms constructed from 1 min of continuous recording. Observations and recording conditions were as follows. (*A*) $I = 0.06$ pA, $i = 0.88$ pA; Static bath; containing forskolin (2 μM), ATP (1 mM), and IBMX (1 mM). (*B*) $I = 1.29$ pA, $i = 0.85$ pA; Static bath as in *A*, with the addition of PKA catalytic subunit (200 u ml^{-1}). (*C*) $I = 0.76$ pA, $i = 0.70$ pA; Perfused bath containing ATP (1 mM), and IBMX (1 mM). (*D*) $I = 0.37$ pA, $i = 0.80$ pA; Perfused bath containing ATP (1 mM), and IBMX (1 mM). (*D*) $I = 0.37$ pA, $i = 0.80$ pA; Perfused bath containing ATP (1 mM). The dashed lines indicate the current level when all channels were closed.

utes both before the addition of PKA and following the removal of PKA. However, IBMX is unable to activate channels in the excised patch configuration as evidenced by the PKA-dependent increase in actively gating channels in the presence of IBMX (Fig. 7, Panels *A* and *B*). Results of this experiment and 8 similar trials are presented in Fig. 8. As shown in Fig. 8*A*, channels continued to actively gate in 65% or more of all patches so long as IBMX was present. PKA neither appeared to further augment the effect of IBMX on channel activity nor did IBMX appear to augment the effect of PKA on ΔF508-CFTR channels. In Fig. 8*B* are shown the effects of IBMX on ΔF508-CFTR channel P_o in the presence and absence of PKA. It is immediately obvious that in the presence of IBMX, the P_o was greater at every time point, although appropriate comparisons did not provide statistical significance with this small data set (4 or 5 patches in each condition). These results suggest a striking divergence in ΔF508-CFTR channel activity due to the presence of IBMX, both in the presence and absence

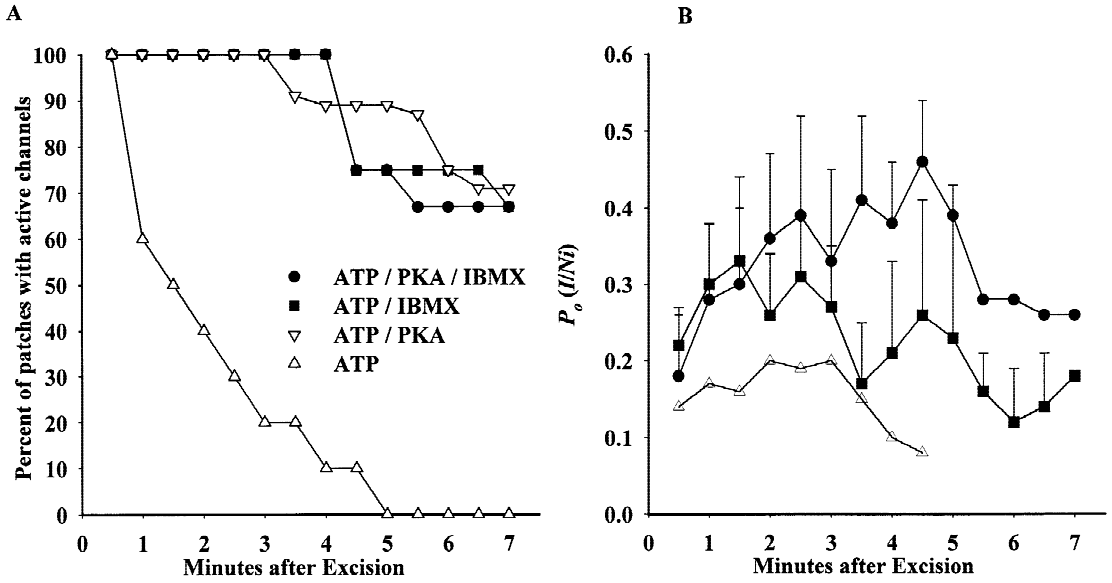

Fig. 8. Time dependence of ΔF508-CFTR channel activity in the absence and presence of IBMX. (*A*) Percentage of patches with channels remaining active in the presence of IBMX (1 mM). Data recorded in the absence of IBMX (previously presented in Fig. 3*A*) is included for direct comparison. (*B*) Comparison of channel P_o in the presence or absence of IBMX. Data recorded in the absence of IBMX (previously presented in Fig. 3*B;* error bars omitted for clarity) is included for direct comparison. Four and five patches were evaluated for effects of IBMX in the absence and presence of PKA, respectively. Means ± SEM are displayed for each data point. SEM could not be determined when the number of patches with actively gating channels fell below three due to breakage of some patches.

of PKA. IBMX increases the duration that ΔF508-CFTR channels remain active following stimulation and appears to increase the P_o of actively gating channels.

Discussion

In the present study, we have shown that the gating behavior of Cl^- channels formed by the most common mutant form of CFTR, ΔF508-CFTR, is distinctly different from that of *wt*-CFTR. Based upon these observations we propose a kinetic model (*see below*) and indicate the transition rates that are most affected by this mutation. Secondarily, we have shown that IBMX has a direct effect on CFTR Cl^- channels, and that this effect can account for at least some of the IBMX-induced stimulation of Cl^- flux in cells expressing this mutant form of the protein as has previously been reported.

Comparisons of ΔF508- and *wt*-CFTR in a Working Kinetic Model

The ΔF508 mutation has been reported to alter the gating behavior of CFTR. Most laboratories have suggested that there is significant difference between these two forms of the protein in macroscopic current or gating behavior (Dalemans et al., 1991; Drumm et al., 1991; Sherry et al., 1994; Becq et al., 1996; Haws et al., 1996; Sato et al., 1996; Hwang et al., 1997) although some reports indicate that ΔF508-CFTR behaves no differently than *wt*-CFTR when reconstituted into similar systems (Li et al., 1993; Pasyk & Foskett, 1995). The reported differences between *wt*- and ΔF508-CFTR could reflect changes in phosphorylation-dependent activation/inactivation and/or changes in nucleotide-dependent gating kinetics. The current results suggest that altered nucleotide-dependent gating activity contributes to an accelerated inactivation of the ΔF508-CFTR channel.

Many kinetic models have been proposed to account for the gating behavior of CFTR when recorded in cell-attached or excised membrane patches and in lipid bilayers. It has now become widely accepted that nucleotide triphosphates are hydrolyzed by CFTR to provide for certain kinetic states to be observed resulting in cyclic kinetic schemes (Gadsby et al., 1994; Gunderson & Kopito, 1995; Bear et al., 1997). Alternatively, simple linear kinetic models have been proposed by ourselves (Venglarik et al., 1994; Schultz et al., 1995) and others (Haws et al., 1992; Fischer & Machen, 1994; Winter et al., 1994) to account for phosphorylation and nucleotide-dependent gating behavior (e.g., Kinetic Scheme 1). Regardless of the model that is employed, it is important to identify open or closed states that are affected by mutations and to determine which states are affected by pharmacological intervention. In the context of the linear scheme which we proposed, the present results support three hypotheses regarding the gating behavior and regulation of ΔF508-CFTR: (i) the general kinetic scheme is

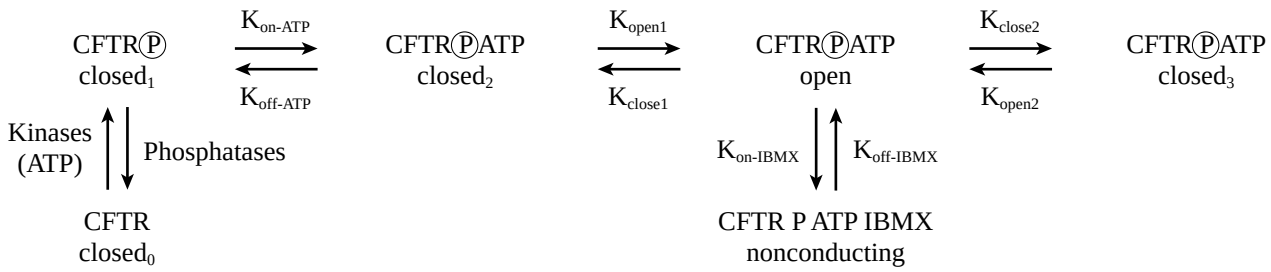

Kinetic Scheme 1

equally applicable for both *wt*- and ΔF508-CFTR, (ii) the nucleotide-dependent opening rate is reduced by the ΔF508 mutation, and (iii) ΔF508-CFTR channels are more likely than *wt*-CFTR to undergo dephosphorylation (i.e., make the $closed_1$ to $closed_0$ transition).

The general kinetic scheme is equally applicable for both *wt*- and ΔF508-CFTR. Results presented in Fig. 1 demonstrate that kinase-dependent stimulation must precede nucleotide-dependent gating. Once activated (phosphorylated), the P_o of ΔF508-CFTR demonstrated an ATP concentration dependence. Although supersaturating concentrations of ATP were not employed in this study, the evidence supports the notion that the maximal ATP-dependent P_o is far from unity, thus requiring the imposition of an ATP-bound, closed state in this scheme ($closed_2$). Truly stationary kinetics were not routinely observed, however first approximations regarding the K_m for ATP, the maximal nucleotide-dependent opening rate, and the closing rate can be made. Results indicate that the K_m is dramatically increased for ΔF508-CFTR compared to our previous observations on *wt*-CFTR evaluated in the same conditions (260 μM *vs.* 24 μM; (Venglarik et al., 1994). If one makes the assumption that 3 mM ATP is sufficient to saturate virtually all nucleotide binding sites, then fluctuation analysis, along with the observed P_o, provides a first approximation of k_{open1} (1.4 ± 0.2 sec^{-1}) and k_{close1} (5.5 ± 0.9 sec^{-1}). These approximations suggest that k_{close1} is not affected by the ΔF508 mutation (6.5 ± 0.5 sec^{-1} for *wt*-CFTR; Venglarik et al., 1994), but that k_{open1} is dramatically reduced (5.4 ± 0.4 sec^{-1} for *wt*-CFTR; Venglarik et al., 1994). Fluctuation analysis also provided parameters that were consistent with previous observations regarding the presence of a short-lived (<2 msec) nonconducting state ($closed_3$). Because of the nature of these transitions and the inability to pharmacologically modify them, the exact location of this state in the kinetic scheme cannot be reliably determined (*see* Venglarik et al., 1994).

Transitions between $closed_0$ and $closed_1$ are oversimplified by Kinetic Scheme 1. Depending upon the expression system and the types of experiments completed, numerous kinases and phosphatases are reported to contribute to the distribution of CFTR between these states such that numerous distinct phosphorylated states are likely to exist. Phosphorylation at numerous known or yet unidentified sites contributes to the likelihood of observing open CFTR channels (Rich et al., 1991; Rich et al., 1993; Gadsby & Nairn, 1994). In the present study, standard conditions as outlined in Materials and Methods were chosen to best approximate those that had been employed in previous studies so that relevant comparisons to *wt*-CFTR could be made. Thus, PKA was employed to activate CFTR channels and specific phosphatase inhibitors were not employed (although F^- was present throughout). These conditions have been shown to provide for stationary, nucleotide-dependent gating behavior of *wt*-CFTR in excised membrane patches of L-cells and T84 cells (Venglarik et al., 1994; Schultz et al., 1995; Schultz et al., 1996). Furthermore, *wt*-CFTR was shown, in the present study, to behave similarly in membrane patches excised from HEK 293 cells.

The nucleotide-dependent P_o of ΔF508-CFTR is significantly reduced when compared to *wt*-CFTR evaluated in excised membrane patches. This observation is consistent with previous reports employing ΔF508-CFTR (Dalemans et al., 1991; Drumm et al., 1991; Sherry et al., 1994; Becq et al., 1996; Haws et al., 1996; Sato et al., 1996; Hwang et al., 1997). However, the mechanisms predicted to account for these differences cannot always be directly compared. For example, Drumm et al. (1991) report that the maximal attainable Cl^- current in *Xenopus* oocytes expressing ΔF508-CFTR was approximately 60% of that elicited in *wt*-CFTR-expressing oocytes. Furthermore, the rate of ΔF508-CFTR activation by a cAMP cocktail was significantly slowed. Likewise, Sato et al. (1996) reported that whole-cell records of Cl^- currents from cells expressing ΔF508-CFTR were significantly smaller than similar cells expressing *wt*-CFTR. While the differences that were reported are significant, the kinetic basis for these observations, at the protein level, could not be assessed in either system. Dalemans et al. (1991) were the first to report that kinetic behavior of ΔF508-CFTR Cl^- channels was different than *wt*-CFTR activity. In both cell attached and excised membrane patches recorded at room temperature, the P_o of ΔF508-CFTR was less than that of *wt*-CFTR. This observation was accounted for by

a fourfold increase in the closed time duration (4.9 sec *vs.* 1.4 sec; unlike the current report, the authors reported a single closed state). Since the recordings were made at room temperature, direct comparisons to the current report cannot be made. It is, however, interesting to note that the authors (Dalemans et al., 1991) reported a loss of channel activity over time; an observation that was reproduced in the current study at more physiological temperatures. Similarly, others have reported that ΔF508-CFTR has an extended closed time compared to *wt*-CFTR when evaluated in cell attached and excised membrane patches at room temperature (Haws et al., 1996; Hwang et al., 1997). In lipid bilayers, Sherry et al. (1994) reported that ΔF508-CFTR had a lower P_o than that of *wt*-CFTR. In this case, though, the reduction in P_o was attributed to a decrease in the burst duration without any difference in the closed duration.

The present observations support and extend previous reports that ΔF508-CFTR has a lower P_o than *wt*-CFTR when recorded in similar conditions. The reduction in P_o is accounted for in two ways. First, in reference to Kinetic Scheme 1, the maximal nucleotide-dependent opening rate (k_{open1}) is reduced by the mutation. At concentrations of ATP which would maximize the likelihood of channels being in the $closed_2$ state, P_o was reduced. This suggests that the conformational change which accompanies ATP binding and results in a conductive state of the channel is slowed by the mutation. The apparent reduction in k_{open1} could be explained by a reduction in $k_{on\text{-}ATP}$—if $k_{off\text{-}ATP}$ is unaffected. This possibility is appealing since it would explain the apparent change in the distribution of channels between $closed_1$ and $closed_2$ which shifted in the favor of $closed_1$ for ΔF508-CFTR. Regardless of which is more affected, $k_{on\text{-}ATP}$ or $k_{off\text{-}ATP}$, the observation remains that the ratio of $k_{off\text{-}ATP}$ to $k_{on\text{-}ATP}$ (i.e., the apparent K_D) is increased by the mutation and the ratio of channels in the $closed_1$ *vs.* the $closed_2$ state is shifted to favor $closed_1$. Thus, because k_{open1} is reduced, after closing to the $closed_2$ state a ΔF508-CFTR channel is more likely to sojourn through $closed_2$ to $closed_1$ before again traversing $closed_2$ to reopen. Furthermore, channels which are in the $closed_1$ state can undergo dephosphorylation to the $closed_0$ state and require kinase-dependent activation before again being available to bind ATP and open. This sojourn through numerous closed states would account for the reduced P_o, the extended closed times, the reduced opening rate, and the requirement for ongoing kinase activity currently observed and previously reported in whole cell, cell attached, and excised membrane patches.

ΔF508-CFTR Dephosphorylates and Inactivates

That PKA could prolong or rescue ΔF508-CFTR channel activity suggests that the active (phosphorylated) form of the mutated protein is less stable than the *wt*-CFTR active form. Because distinct phospho-forms of CFTR have been associated with channel activity (Gadsby & Nairn, 1994), the data suggest that one or more of the phosphorylation sites that is keenly important for gating activity is adversely affected by the ΔF508 mutation. That the maximum P_o achieved by ΔF508-CFTR was less than observed for *wt*-CFTR in these conditions might suggest that ΔF508-CFTR is not able to be as highly phosphorylated; that one or more sites are not kinase accessible. If dephosphorylation leads to inactivation, then a channel with fewer phosphorylated sites might be expected to inactivate more rapidly as was observed. Experiments employing *wt*-CFTR led us to conclude that the apparent instability of the phosphorylated form could, in part, be due to reduced ATP affinity. Indeed, we showed that absence of ATP in the cytoplasmic bath accelerates inactivation of *wt*-CFTR. These results suggest that, upon interaction with nucleotides, the first NBD interacts with other domains to 'protect' one or more phosphorylated residues. Furthermore, the results suggest that either CFTR auto-dephosphorylates, or a phosphatase is present in the excised membrane patch and able to inactivate CFTR when the first NBD is not protecting the necessary site(s). This observation is bolstered by previous reports suggesting that the R-domain intimately associates with the NBD (Ma et al., 1997; Winter & Welsh, 1997; Matthews et al., 1998). In these reports, changes in phosphorylation of the R-domain resulted in changes in ATP-sensitivity. Presently, we show that the converse can also be true; changes in ATP sensitivity due to mutations in the NBD result in changes in the stability of phosphorylation state(s). The current observations do not address questions regarding the phosphatases that participate or are most important for the inactivation of CFTR. Rather they merely indicate that a de-activation mechanism is present in the excised membrane patch and that this mechanism is inhibited by the presence of ATP.

IBMX Directly Modifies CFTR Channel Activity

Numerous laboratories have reported that IBMX favorably affects ΔF508-CFTR Cl^- channel activity and various mechanisms have been proposed. In most cases IBMX is employed as a nonspecific inhibitor of cAMP phosphodiesterase activity to increase and maintain high levels of kinase activity within the cell. Depending upon the cell type, the type of PDE present, and the activity of the PDE, different sensitivities to IBMX are expected (Beavo, 1995). Additionally, IBMX may act at other sites within the cell at the concentrations being employed to stimulate ΔF508-CFTR (e.g., phosphatase inhibition).

Alternative mechanisms for the stimulation of ΔF508-CFTR by IBMX have been proposed. Drumm et

al. (1991) first reported that IBMX, at concentrations approaching solution saturation, stimulated Cl^- conductance in *Xenopus* oocytes expressing ΔF508-CFTR. The authors attributed this phenomena to inhibition of cAMP phosphodiesterase resulting in concentrations of cAMP that could not otherwise be attained in this expression system. A direct effect of IBMX on CFTR was not imputed at that time although subsequent reports from this laboratory (Wilkinson et al., 1996, 1997) have incorporated an IBMX-induced amplitude reduction term into their macroscopic kinetic calculations. Yang et al. (1993) reported that 4 mM IBMX, but not 0.1 mM IBMX, would stimulate halide conductance in fibroblasts expressing ΔF508-CFTR. It is particularly intriguing that stimulation could occur in cells incubated at a nonpermissive temperature, (37°C) suggesting that a pool of ΔF508-CFTR was present at the cell membrane. Likewise, Haws et al. (1996) reported that IBMX, when used at 5 mM but not at 0.1 mM, stimulated halide efflux from cells expressing ΔF508-CFTR. In each case, the mechanism of stimulation at the level of the channel was not determined although the authors speculated that there might be a direct interaction of IBMX with mutant forms of CFTR. In evaluating membrane patches, Becq et al. (1993, 1994) reported that IBMX reduced the channel rundown accompanying patch excision. Based upon the effects of other drugs (e.g., (−)-*p*-bromotetramisole), the authors concluded that the effect of IBMX was mediated, at least in part, by the inhibition of a phosphatase(s) which inactivated CFTR. Recently, these authors (Chappe et al., 1998) reported that various xanthine derivatives stimulated CFTR-mediated anion flux without affecting intracellular cAMP concentration. The xanthine rank order of potency for anion flux stimulation was unique when compared to that for either phosphodiesterase inhibition or adenosine receptor antagonism. Thus, an apparently unique functional binding site for xanthines was identified. However, whether the functional site was on CFTR remained unresolved. The current data indicates that IBMX can interact directly with CFTR as has been reported for other xanthines (Arispe et al., 1998). The exact physical location of the functionally relevant binding site remains to be determined although a direct interaction with NBD1 has been reported (Cohen et al., 1997). In this regard, mutations in either the R-domain (Wilkinson et al., 1997) or the NBDs (Smit et al., 1993) changed the sensitivity to IBMX when assayed in *Xenopus* oocytes. Whether these mutations reflect distinct changes in an IBMX binding site or domain interactions remains to be determined.

The current data show that IBMX has a direct effect on both *wt*- and ΔF508-CFTR channel activity. Importantly, the results indicate that a distinct conformational state, the open state, is the primary target. In Kinetic Scheme 1, CFTR can exist in the open state of any one of four closed states in the absence of IBMX. Exposure to IBMX provides an additional nonconductive state in which CFTR can reside. Because the IBMX-induced non-conducting state communicates only with the open state, the state distribution is shifted to favor open state occupancy and away from inactivation (i.e., away from $closed_0$ and the state(s) that directly communicates with $closed_0$). For *wt*-CFTR, where transitions from the $closed_1$ to the $closed_0$ state were seldom observed, the effect of IBMX was simply to prolong the open bursts and diminish the observed channel amplitude. IBMX induced no significant changes in macroscopic current. However, for ΔF508-CFTR the effect of altering the state distribution was more profound. The presence of the IBMX-bound state reduces the proportion of channels in the $closed_2$ state and thus the proportion of channels that can sojourn through $closed_1$ and dephosphorylate is reduced. IBMX not only extended the burst duration, but also reduced the transition rate to the $closed_0$ state.

In summary, we have shown that the phosphorylation- and nucleotide-dependent gating behavior of ΔF508-CFTR is qualitatively similar to, but quantitatively different from that of *wt*-CFTR. When compared to *wt*-CFTR, ΔF508-CFTR has reduced ATP sensitivity, reduced maximal P_o and is more likely to inactivate. The reduced ATP sensitivity contributes to instability of the activated form. IBMX has direct and significant effects on both *wt*- and ΔF508-CFTR. The drug interacts with the activated, nucleotide-bound and open form of CFTR to introduce a short-lived nonconducting state. Secondarily, the interaction with IBMX stabilizes the nucleotide-bound form of ΔF508-CFTR and thus prevents inactivation. This effect of IBMX on ΔF508-CFTR helps to explain the encouraging 'therapeutic' effects that have been observed in model systems. Furthermore, these observations introduce this conformational state of CFTR as a distinct therapeutic target for pharmaceutical development as we design compounds to reduce or preclude suffering of cystic fibrosis patients.

Portions of the work were completed by the authors at the University of Alabama at Birmingham, Department of Physiology and Biophysics and Gregory Fleming James Cystic Fibrosis Research Center. The authors extend their thanks to Harris Jerdon and Heather Balombiny for their technical assistance.

Deep and sincere appreciation is extended to A. Keith Glaubius and his family for their support of this work. His guidance, insight and encouragement could be provided by no other mentor.

Supported by National Institutes of Health (DK-38518, DK-45970, DK-08846) and the Cystic Fibrosis Foundation (I848).

References

Arispe, N., Ma, J., Jacobson, K.A., Pollard, H.B. 1998. Direct activation of cystic fibrosis transmembrane conductance regulator chan-

nels by 8-cyclopentyl-1,3-dipropylxanthine (CPX) and 1, 3-diallyl-8-cyclohexylxanthine. *J. Biol. Chem.* **273:**5727–5734

Bear, C.E., Li, C., Galley, K., Wang, Y., Garami, E., Ramjeesingh, M. 1997. Coupling of ATP hydrolysis with channel gating by purified, reconstituted CFTR. *J. Bioenerg. Biomembr.* **29:**465–473

Beavo, J.A. 1995. Cyclic nucleotide phosphodiesterases: Functional implications of multiple isoforms. *Physiol. Rev.* **75:**725–748

Beavo, J.A., Rogers, N.L., Crofford, O.B., Hardman, J.G., Sutherland, E.W., Newman, E.V. 1970. Effects of xanthine derivatives on lipolysis and on adenosine 3′,5′-monophosphate phosphodiesterase activity. *Mol. Pharmacol.* **6:**597–603

Becq, F., Fanjul, M., Merten, M., Figarella, C., Hollande, E., Gola, M. 1993. Possible regulation of CFTR-chloride channels by membrane-bound phosphatases in pancreatic duct cells. *FEBS Lett.* **327:**337–342

Becq, F., Jensen, T.J., Chang, X., Savoia, A., Rommens, J.M., Tsui, L., Buchwald, M., Riordan, J.R., Hanrahan, J.W. 1994. Phosphatase inhibitors activate normal and defective CFTR chloride channels. *Proc. Natl. Acad. Sci. USA* **91:**9160–9164

Becq, F., Verrier, B., Chang, X.B., Riordan, J.R., Hanrahan, J.W. 1996. cAMP- and Ca^{2+}-independent activation of cystic fibrosis transmembrane conductance regulator channels by phenylimidazothiazole drugs. *J. Biol. Chem.* **271:**16171–16179

Berger, H.A., Anderson, M.P., Gregory, R.J., Thompson, S., Howard, P.W., Maurer, R.A., Mulligan, R., Smith, A.E., Welsh, M.J. 1991. Identification and regulation of the cystic fibrosis transmembrane conductance regulator-generated chloride channel. *J. Clin. Invest.* **88:**1422–1431

Berger, H.A., Travis, S.M., Welsh, M.J. 1998. Fluoride stimulates cystic fibrosis transmembrane conductance regulator Cl^- channel activity. *Am. J. Physiol.* **274:**L305–L312

Brooks, S.P., Storey, K.B. 1992. Bound and Determined: a computer program for making buffers of defined ion concentrations. *Anal. Biochem.* **201:**119–126

Brown, C.R., Hong-Brown, L.Q., Biwersi, J., Verkman, A.S., Welch, W.J. 1996. Chemical chaperones correct the mutant phenotype of the ΔF508 cystic fibrosis transmembrane conductance regulator protein. *Cell Stress & Chaperones* **1**:117–125

Chappe, V., Mettey, Y., Vierfond, J.M., Hanrahan, J.W., Gola, M., Verrier, B., Becq, F. 1998. Structural basis for specificity and potency of xanthine derivatives as activators of the CFTR chloride channel. *Br. J. Pharmacol.* **123:**683–693

Cheng, S.H., Gregory, R.J., Marshall, J., Paul, S., Souza, D.W., White, G.A., O'Riordan, R.R., Smith, A.E. 1990. Defective intracellular transport and processing of CFTR is the molecular basis of most cystic fibrosis. *Cell* **63:**827–834

Cohen, B.E., Lee, G., Jacobson, K.A., Kim, Y.C., Huang, Z., Sorscher, E.J., Pollard, H.B. 1997. 8-cyclopentyl-1,3-dipropylxanthine and other xanthines differentially bind to the wild-type and delta F508 first nucleotide binding fold (NBF-1) domains of the cystic fibrosis transmembrane conductance regulator. *Biochemistry* **36:**6455–6461

Croce, M.A., Kramer, G.L., Garbers, D.L. 1979. Inhibition of alkaline phosphatase by substituted xanthines. *Biochem. Pharmacol.* **28:**1227–1231

Dalemans, W., Barbry, P., Champigny, G., Jallat, S., Dott, K., Dreyer, D., Crystal, R.G., Pavirani, A., Lecoq, J.-P., Lazdunski, M. 1991. Altered chloride ion channel kinetics associated with the ΔF508 cystic fibrosis mutation. *Nature* **354:**526–528

Denning, G., Anderson, M., Amara, J., Marshall, J., Smith, A., Welsh, M. 1992. Processing of mutant cystic fibrosis transmembrane conductance regulator is temperature-sensitive. *Nature* **358:**761–764

Drumm, M.L., Wilkinson, D.J., Smit, L.S., Worrell, R.T., Strong, T.V., Frizzell, R.A., Dawson, D.C., Collins, F.S. 1991. Chloride conductance expressed by delta F508 and other mutant CFTRs in *Xenopus* oocytes. *Science* **254:**1797–1799

Farley, J.R., Ivey, J.L., Baylink, D.J. 1980. Human skeletal alkaline phosphatase. Kinetic studies including pH dependence and inhibition by theophylline. *J. Biol. Chem.* **255:**4680–4686

Fischer, H., Machen, T.E. 1994. CFTR displays voltage dependence and two gating modes during stimulation. *J. Gen. Physiol.* **104:**541–566

Gadsby, D.C., Hwang, T.C., Baukrowitz, T., Nagel, G., Horie, M., Nairn, A.C. 1994. Regulation of CFTR channel gating. *Jpn. J. Physiol.* **44, Suppl. 2:**S183–S192

Gadsby, D.C., Nairn, A.C. 1994. Regulation of CFTR channel gating. *Trends Biochem. Sci.* **19:**513–518

Graham, F.L., van Der Eb, A.J. 1973. A new technique for the assay of infectivity of human adenovirus 5 DNA. *Virology* **52:**456–467

Gunderson, K.L., Kopito, R.R. 1995. Conformational states of CFTR associated with channel gating: the role of ATP binding and hydrolysis. *Cell* **85:**231–239

Haws, C., Krouse, M.E., Xia, Y., Gruenert, D.C., Wine, J.C. 1992. CFTR channels in immortalized human airway cells. *Am. J. Physiol.* **263:**L692–L707

Haws, C.M., Nepomuceno, I.B., Krouse, M.E., Wakelee, H., Law, T., Xia, Y., Nguyen, H., Wine, J.J. 1996. Delta F508-CFTR channels: kinetics, activation by forskolin, and potentiation by xanthines. *Am. J. Physiol.* **270:**C1544–C1555

He, Z., Raman, S., Guo, Y., Reenstra, W.W. 1998. Cystic fibrosis transmembrane conductance regulator activation by cAMP-independent mechanisms. *Am. J. Physiol.* **275:**C958–C966

Horn, R. 1991. Estimating the number of channels in patch recordings. *Biophys. J.* **60:**433–439

Hwang, T.-C., Wang, F., Yang, I.C.-H., Reenstra, W.W. 1997. Genistein potentiates wild-type and ΔF508-CFTR channel activity. *Am. J. Physiol.* **273:**C988–C998

Li, C., Ramjeesingh, M., Reyes, E., Jensen, T., Chang, X., Rommens, J.M., Bear, C.E. 1993. The cystic fibrosis mutation (ΔF508) does not influence the chloride channel activity of CFTR. *Nat. Genet.* **3:**311–316

Ma, J., Zhao, J., Drumm, M.L., Xie, J., Davis, P.B. 1997. Function of the R domain in the cystic fibrosis transmembrane conductance regulator chloride channel. *J. Biol. Chem.* **272:**28133–28141

Matthews, C.J., Tabcharani, J.A., Chang, X.-B., Jensen, T.J., Riordan, J.R., Hanrahan, J.W. 1998. Dibasic protein kinase A sites regulate bursting rate and nucleotide sensitivity of the cystic fibrosis transmembrane conductance regulator chloride channel. *J. Physiol.* **508:**365–377

Pasyk, E.A., Foskett, J.K. 1995. Mutant (delta F508) cystic fibrosis transmembrane conductance regulator Cl^- channel is functional when retained in endoplasmic reticulum of mammalian cells. *J. Biol. Chem.* **270:**12347–12350

Rich, D.P., Berger, H.A., Cheng, S.H., Travis, S.M., Saxena, M., Smith, A.E., Welsh, M.J. 1993. Regulation of the cystic fibrosis transmembrane conductance regulator Cl^- channel by negative charge in the R domain. *J. Biol. Chem.* **268:**20259–20267

Rich, D.P., Gregory, R.J., Anderson, M.P., Manavalan, P., Smith, A.E., Welsh, M.J. 1991. Effect of deleting the R domain on CFTR-generated chloride channels. *Science* **253:**205–207

Sato, S., Ward, C., Krouse, M., Wine, J., Kopito, R. 1996. Glycerol reverses the misfolding phenotype of the most common cystic fibrosis mutation. *J. Biol. Chem.* **271:**635–638

Schultz, B.D., Bridges, R.J., Frizzell, R.A. 1994. IBMX-induced fast

block of CFTR can explain stimulation of ΔF508-CFTR. *Pediatr. Pulmonol. Suppl.* **10:**205

Schultz, B.D., Bridges, R.J., Frizzell, R.A. 1996. Lack of conventional ATPase properties in CFTR chloride channel gating. *J. Membrane Biol.* **151:**63–75

Schultz, B.D., Frizzell, R.A., Bridges, R.J. 1994. IBMX stabilizes the ATP-bound state of ΔF508-CFTR. *J. Gen. Physiol.* **104:**35

Schultz, B.D., Venglarik, C.J., Bridges, R.J., Frizzell, R.A. 1995. Regulation of CFTR Cl^- channel gating by ADP and ATP analogues. *J. Gen. Physiol.* **105:**329–361

Sherry, A.M., Cuppoletti, J., Malinowska, D.H. 1994. Differential acidic pH sensitivity of ΔF508 CFTR Cl^- channel activity in lipid bilayers. *Am. J. Physiol.* **266:**C870–C875

Smit, L.S., Wilkinson, D.J., Mansoura, M.K., Collins, F.S., Dawson, D.C. 1993. Functional roles of the nucleotide-binding folds in the activation of the cystic fibrosis transmembrane conductance regulator. *Proc. Natl. Acad. Sci. USA* **90:**9963–9967

Tabcharani, J.A., Chang, X.-B., Riordan, J.R., Hanrahan, J.W. 1991. Phosphorylation-regulated Cl^- channel in CHO cells stably expressing the cystic fibrosis gene. *Nature* **352:**628–631

Venglarik, C.J., Schultz, B.D., Frizzell, R.A., Bridges, R.J. 1994. ATP alters current fluctuations of cystic fibrosis transmembrane conductance regulator: Evidence for a three-state activation mechanism. *J. Gen. Physiol.* **104:**123–146

Welsh, M.J., Smith, A.E. 1993. Molecular mechanisms of CFTR chloride channel dysfunction in cystic fibrosis. *Cell* **73:**1251–1254

Wilkinson, D.J., Mansoura, M.K., Watson, P.Y., Smit, L.S., Collins, F.S., Dawson, D.C. 1996. CFTR: the nucleotide binding folds regulate the accessibility and stability of the activated state. *J. Gen. Physiol.* **107:**103–119

Wilkinson, D.J., Strong, T.V., Mansoura, M.K., Wood, D.L., Smith, S.S., Collins, F.S., Dawson, D.C. 1997. CFTR activation: additive effects of stimulatory and inhibitory phosphorylation sites in the R domain. *Am. J. Physiol.* **273:**L127–L133

Winter, M.C., Sheppard, D.N., Carson, M.R., Welsh, M.J. 1994. Effect of ATP concentration on CFTR Cl^- channels: a kinetic analysis of channel regulation. *Biophys. J.* **66:**1398–1403

Winter, M.C., Welsh, M.J. 1997. Stimulation of CFTR activity by its phosphorylated R domain. *Nature* **389:**294–296

Yang, Y., Devor, D.C., Engelhardt, J.F., Ernst, S.A., Strong, T.V., Collins, F.S., Cohn, J.A., Frizzell, R.A., Wilson, J.M. 1993. Molecular basis of defective anion transport in L cells expressing recombinant forms of CFTR. *Hum. Mol. Genet.* **2:**1253–1261